Finite Element Study of Multilayer Surfacing Systems on Orthotropic Steel Bridges

J. Li[1] , X. Liu[2], A. Scarpas[3] & G. Tzimiris[4]

[1]Road and Railway Engineering, Faculty of Civil Engineering and Geosciences, Delft University of Technology, Stevinweg 1, 2628 CN Delft, The Netherlands; email: Jinlong.Li@tudelft.nl
[2] Road and Railway Engineering, Faculty of Civil Engineering and Geosciences, Delft University of Technology, Stevinweg 1, 2628 CN Delft, The Netherlands; email: X.Liu@tudelft.nl
[3] Road and Railway Engineering, Faculty of Civil Engineering and Geosciences, Delft University of Technology, Stevinweg 1, 2628 CN Delft, The Netherlands; email: a.scarpas@tudelft.nl
[3] Road and Railway Engineering, Faculty of Civil Engineering and Geosciences, Delft University of Technology, Stevinweg 1, 2628 CN Delft, The Netherlands; email: G.Tzimiris@tudelft.nl

ABSTRACT

Light weight orthotropic steel bridge decks have been widely utilized for bridges in seismic zones, movable bridges and long span bridges. In the last three decades, severe problems were reported in relation to asphaltic surfacing materials on orthotropic steel deck bridges. Earlier investigations have shown that the bonding strength of membrane layers to the surrounding materials has a strong influence on the structural response of orthotropic steel bridge decks. The most important requirement for the application of membrane materials on orthotropic steel bridge decks is that the membrane adhesive layer shall be able to provide sufficient bond to the surrounding materials. The research aims on developing a FE tool to simulate and understand the performance of asphaltic surfacing structures, so as to improve the design of surfacings and increase their service life. In this paper, Finite Element (FE) simulations of Merwedebrug bridge with two membrane layers system are presented. The finite element system CAPA-3D developed at the Section of Structural Mechanics of TU Delft has been utilized as the numerical platform for this study. Due to the multilayer of the surfacing materials and geometrical complexity of the steel bridge, the FE model shows the in time development of strains and stresses inside the surfacing materials depends highly on the wheel loading frequency, wheel position, membrane bonding strength as well as thicknesses and characteristics of the surfacing layers. Emphasis is placed on the distribution of strains and the evolution of damage in surfacing layers of different cases. Recommendations of surfacing structures design on orthotropic steel bridges are given.

Keywords: orthotropic steel deck bridges, FE simulation, multilayer sufacing systems, membranes.

1 INTRODUCTION

Since the first orthotropic steel bridge (OSB) was open for use in 1950 over the Neckar River in Mannheim, Germany, the OSB becomes a popular economical alternative when the following issues are important: lower mass, ductility, thinner or shallower sections, rapid bridge installation, and cold-weather construction[1]. Lower superstructure mass is the primary reason for the use of orthotropic decks in long-span bridges. Very thin decks can be built using the orthotropic system. In the Netherlands, the first orthotropic steel bridges were the Hartel bridge and the Harmsen bridge which opened in 1968. Nowadays more than 1000 orthotropic steel bridges have been built in Europe, out of which 86 are in the Netherlands. In Asia, there are also several orthotropic steel bridges and some are currently being built, especially in China and Japan [2].

In the Netherlands, an asphaltic surfacing for orthotropic steel bridge decks mostly consists of two structural layers. The upper layer consists of Porous Asphalt (PA) because of its good noise

reduction characteristics. For the lower layer a choice between Mastic Asphalt (MA) or Guss Aspahlt (GA) are utilized. Mostly, different membrane layers are involved, functioning as bonding and water proofing layers. A typical layout of an orthotropic bridge with open stiffeners in the Netherlands is shown in Figure 1.

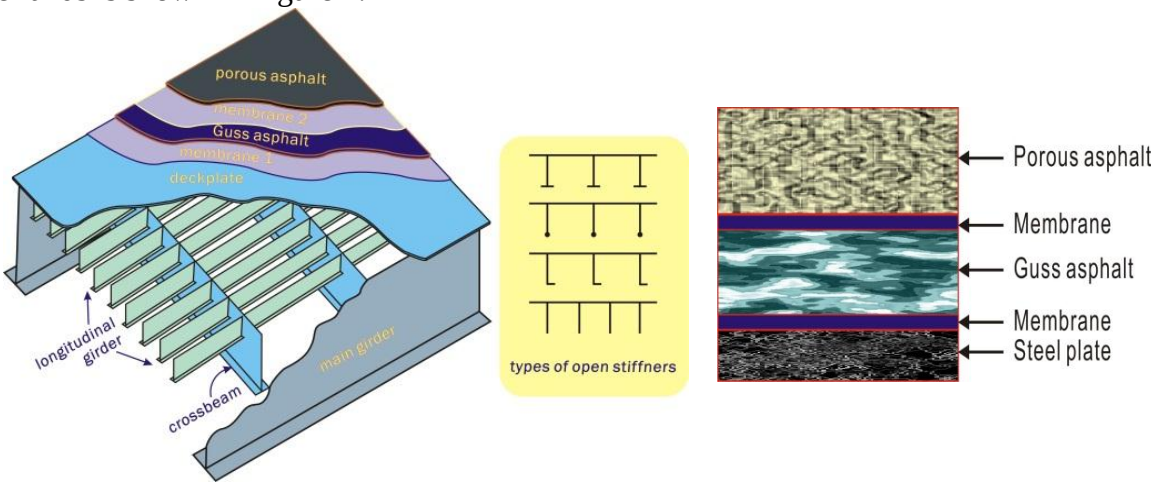

Figure 1 A typical layout of an OSDB with two-layer surfacing system

In the last three decades, several problems were reported in relation to asphaltic surfacing materials on orthotropic steel deck bridges such as rutting, cracking, loss of bond between the surfacing material and the steel plate. Better understanding of the response of the multilayer surfacings is required in order to improve the current design methodologies aimed at prolonging the service life of the wearing course.

This study aims at providing a better understanding of multilayer surfacing systems based on composite beam theory and FEM simulations. The objective is to optimize multilayer surfacing systems composed of various asphaltic mixes and two layers of membranes. Special attention is paid on the influence of the characteristics of the interface regions between the various components. Finally, guidelines are provided for engineers involved with this type of constructions.

After a brief presentation of material models of surfacing materials, FE simulations of the Dutch Merwede bridge are presented. The finite element system CAPA-3D[3] developed at the Section of Structural Mechanics of TU Delft has been utilized as the numerical platform for this study.

The interaction between two bituminous mix surfacings, two membranes are quantified systematically. Representative material properties are utilized to describe the mechanical behavior of all material layers. The FE results show that, due to the multilayer nature of the surfacings and the geometric complexity of the steel bridge, the development of strains and stresses depends highly on the traffic loading frequency, wheel position, membrane bonding characteristics as well as the thicknesses and characteristics of the surfacing layers.

2 MATERIAL MODELS AND PARAMETERS OF SURFACING MATERIALS

2.1 Asphaltic materials

As shown in Figure 1, there are four layers of asphalt materials: porous asphalt, guss asphalt, upper and bottom membrane layers. The mechanical characteristics of those asphalt material layers are different with the steel deck plate. It is well known that the asphaltic materials show nonlinear behavior. It is necessary to describe the real response of the surfacing materials in order to correctly understand the response the surfacing systems.

It is believed that a viscoelastic material model, which can capture the main features of the mechanical behavior of asphaltic materials of orthotropic steel bridge is certainly needed. The viscoelastic Zener model is utilized for this finite element study. The reason of choosing the generalization of the Zener model for this finite element is because its constitutive relation is simple

and the model parameter can be easily determined by the conventional experimental tests, i.e. creep test or relaxation test. Figure 2 shows the mechanical analog of this viscoelastic Zener model.

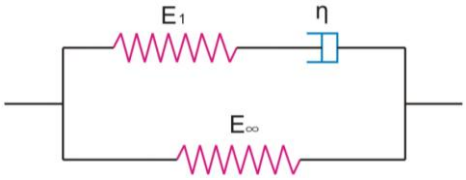

Figure 2 Schematic diagram of Zener model

The model consists of two parallel components. One is purely elastic with modulus E_∞ and the other is viscoelastic consisting of a spring with modulus E_1 and a damper with viscosity coefficient η in series.

The governing equations of Zener model are listed as follows

$$\sigma = E_\infty \varepsilon + E_1 (\varepsilon - \varepsilon_v) \tag{1}$$

$$E_1 (\varepsilon - \varepsilon_v) = \eta_1 \dot{\varepsilon}_v \tag{2}$$

$$\varepsilon_v = \varepsilon(t) - \varepsilon(0)\exp\left(-\frac{E_1}{\eta_1} t\right) - \int_0^t \exp\left(-\frac{E_1}{\eta_1}(t-\tau)\right)\dot{\varepsilon}(\tau)\,d\tau \tag{3}$$

where $\varepsilon(0)$ is the strain in time zero.

2.2 Interface layers

A contact interface element based on the previous work by Liu & Scarpas[4] within the FE package CAPA-3D is utilized to model the cohesive behavior of the membranes and the surrounding surfacing materials causing into contact.

The contact interface element developed is based on the classical 16-noded interface element. It consists of two opposite faces each with 8 nodes. The thickness of the element in its un-deformed configuration can be specified to any initial value.

A cohesive traction-separation law is utilized to prevent the contact interface to freely separate as soon as it undergoes tensile forces, see Figure 3.

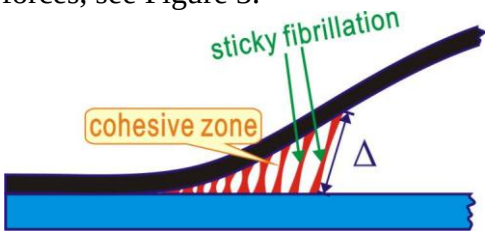

Figure 3 Schematic of traction separation at contact interface

Interfacial fibrillation is a typical mechanism that frequently occurs during debonding of membranes from substrates, Figure 3. It involves large displacements at the interface as well as large deformations in the membrane material. Therefore, a generic cohesive zone model is introduced that is suitable to describe the process of membrane debonding from the substrate.

The cohesive zone law which is utilized to describe the traction-separation relation of fibrillation is controlled by one constitutive relation between traction force and the opening displacement along the fibril axis, Figure 3. Under large displacements, it is no longer physical to discriminate between normal and tangential openings. In the case of membrane debonding from substrates, such large displacements are bridged by fibrils, which at more or less like non-linear springs that can only transfer load along their axis.

The cohesive law proposed here is defined as:

$$T = \frac{G_c}{\delta_c}\left(\frac{\Delta}{\delta_c}\right)\exp\left(-\frac{\Delta}{\delta_c}\right) \tag{4}$$

where G_c is the strain energy release rate which is characterized as the energy per unit crack length required for crack/debonding extension. δ_c is a characteristic opening length. The maximum traction f_t is related to G_c and δ_c, see Figure 4.

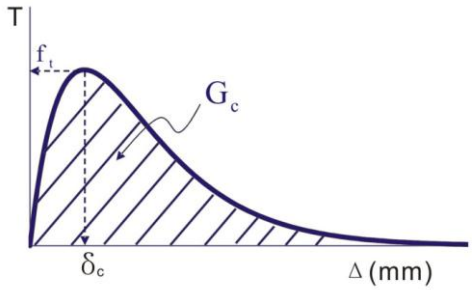

Figure 4 Schematic traction-separation relation

3 FINITE ELEMENT SIMULATIONS OF THE MERWEDE BRIDGE

3.1 FE mesh and material properties

The Merwede bridge, locates in the A27 near Gorinchem, was opened on March 15 1961 by Queen Juliana. Over the past fifty years, this bridge has been playing very important role in connecting traffic between Randstad and North Brabant. Over 100,000 vehicles pass through the bridge every day as well as many cyclists. The Merwede bridge steel deck was constructed with open longitudinal stiffeners placed each 300mm. Crossbeams were placed every 2m and with 10mm thick steel deck plate, Figure 5.

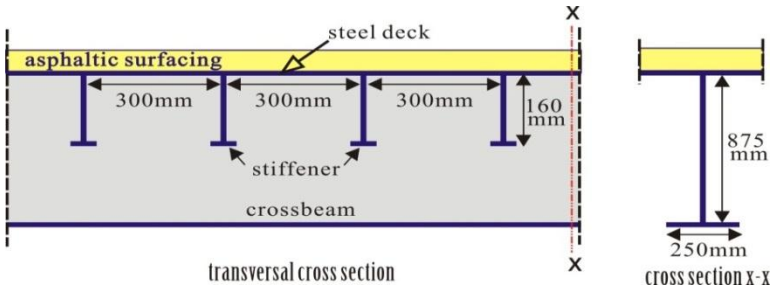

Figure 5 Transverse cross-section of the Merwede bridge

FE analyses was performed to better understand the composite behavior of the multilayer surfacing system. The FE mesh with symmetry in a vertical plane perpendicular to the direction of the bridge span is illustrated in Figure 6. A dual wheel moving load with 80km/h is applied on the top layer of the asphalt concrete. The moving load location and boundary conditions are shown in Figure 7.

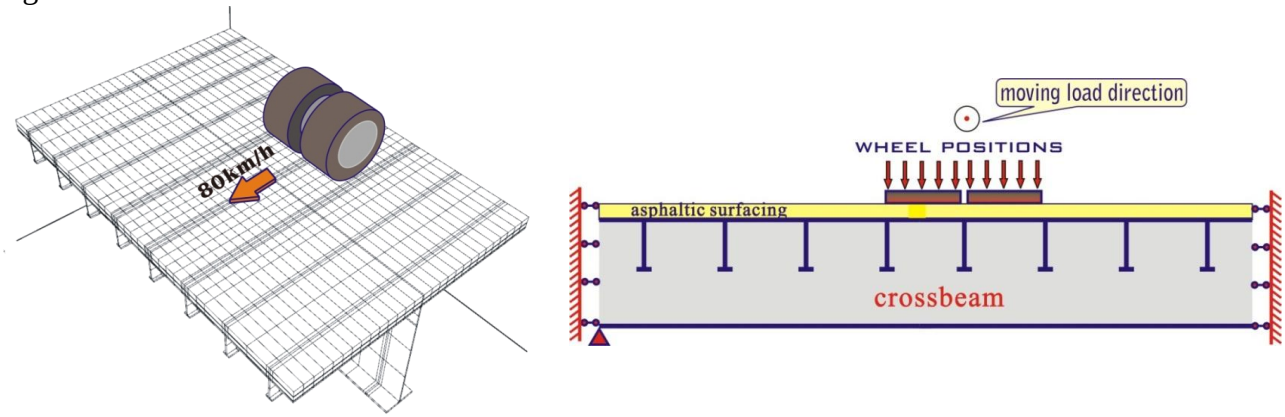

Figure 6 The mesh for simulation of moving load

Figure 7 Cross section of the moving load location and boundary conditions

In this study, all four contact interface regions are utilized in the simulation of the bonding between the various surfacing materials. Steel is regarded as a linear elastic material with Young's modulus 210000 MPa and Poisson's ratio 0.2. Asphaltic surfacings and membranes are assumed to be viscoelastic. Details of the finite element layers are shown in Figure 8.

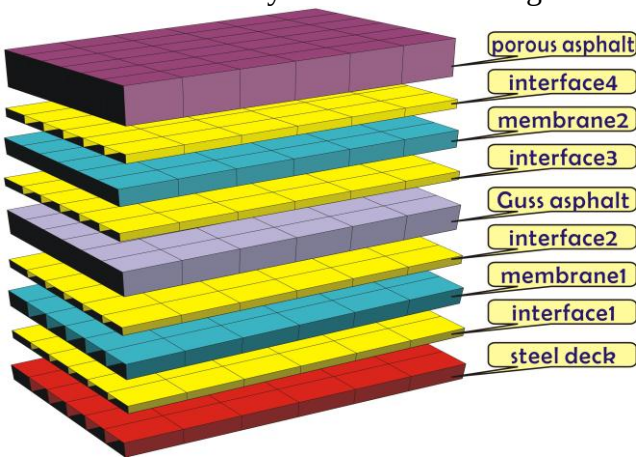

Figure 8 Finite element layers of bridge surfacing system

The mechanical properties of the surfacing materials are temperature dependent. All the studied cases were simulated under $10^{\circ}C$ and $-5^{\circ}C$ respectively. The parameters for porous asphalt and guss asphalt at $10^{\circ}C$ and $-5^{\circ}C$ are shown in Table 1. Four different surfacing structures are simulated. Five membrane products named A1, A2, B, C1and C2 are involved in those surfacing systems. The material properties of those five membrane products at $10^{\circ}C$ and $-5^{\circ}C$ are listed in Table 2.

Table 1 Parameters of porous asphalt and guss asphalt ($10^{\circ}C$ & $-5^{\circ}C$)

temperature ($^{\circ}C$)	material layer	E1(MPa)	E_{∞} (MPa)	Poisson's ratio	η (MPa.s)
10	Porous asphalt	200	1	0.3	15750
	Guss asphalt	450	3	0.3	15750
-5	Porous asphalt	2000	10	0.3	22500
	Guss asphalt	4500	30	0.3	22500

Table 2 Properties of the five membrane products at $+10^0C$ and -5^0C

temperature($^{\circ}C$)	Property	A1	A2	B	C1	C2
10	E1	6.19	5.7	4.59	9.24	9.38
	Poisson's ratio	0.15	0.15	0.15	0.15	0.15
	eta η	1876	1911	192	336.65	475.65
	E∞	5.045	4.38	2.962	16.215	4.8
-5	E1	61.9	57	45.9	92.4	93.8
	Poisson's ratio	1.5	1.5	1.5	1.5	1.5
	eta η	18760	19110	1920	3366.5	4756.5
	E∞	50.45	43.8	29.62	162.15	48

Figure 9 shows a schematic overview of the FE simulation plan of this section.

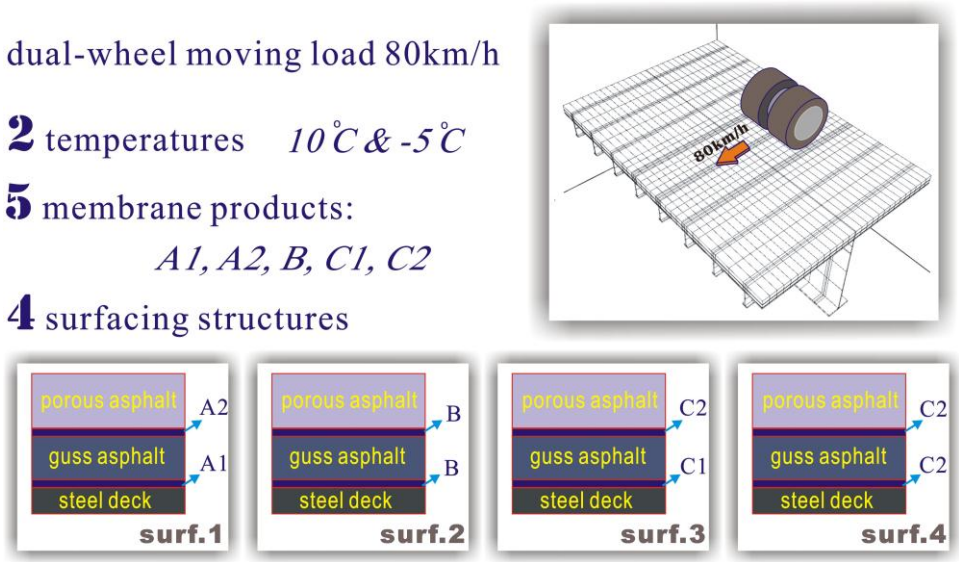

Figure 9 FE simulation plan of a moving load submitted to different surfacing systems

3.2 Responses of the bridge with various surfacing structures

The one-way moving load was simulated for 1000 cycles. A typical in time transversal strain of a point in the bottom membrane layer is plotted in Figure 10.

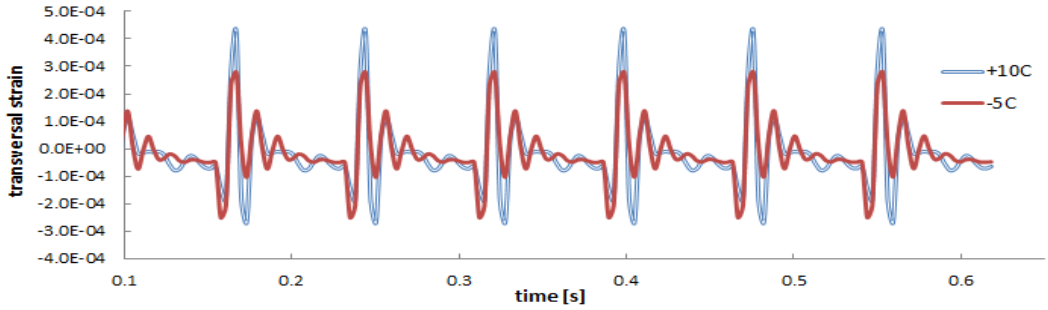

Figure 10 In time transversal strain at different temperatures

From Figure 10, the development of transversal strains as the wheel moves can be seen. The dynamic response of the surfacing structure at 10 °C is clearly higher than that at -5 °C.

Figure 11 shows the overall distribution of transversal strains in the structure due to the passage of the moving load.

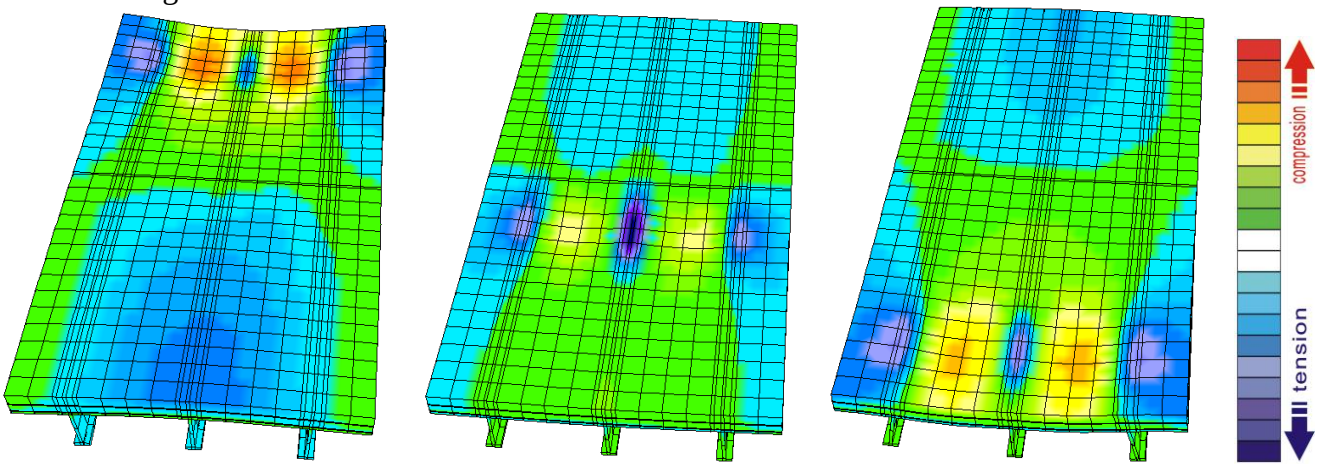

Figure 11 Transversal strains at different positions of the moving load

It can be observed that high tensile strains occur in the middle of the dual-wheel load as well as along its two sides, on top of the stiffeners. The highest transversal compressive strains occur when

the load is right between two crossbeams, while the highest transversal tensile strains appear when the wheel is next to the crossbeam. The bottom membrane sustains both higher tensile and compressive strains than the top membrane does. This phenomenon could be explained by stress/strain concentrations because the lower membrane layer is closer to bridge stiffeners so that stronger concentrations are achieved. Rather high tensile strain around 2000 μm/m occurs at the top of the surfacing from moving load simulations (Figure 11) and when the temperature increases, the accompanying decrease in mix stiffness results to significantly higher strain.

The developments of the maximum transversal strains in the four surfacing structures at +10°C and -5 °C are plotted in Figure 12 and 13.

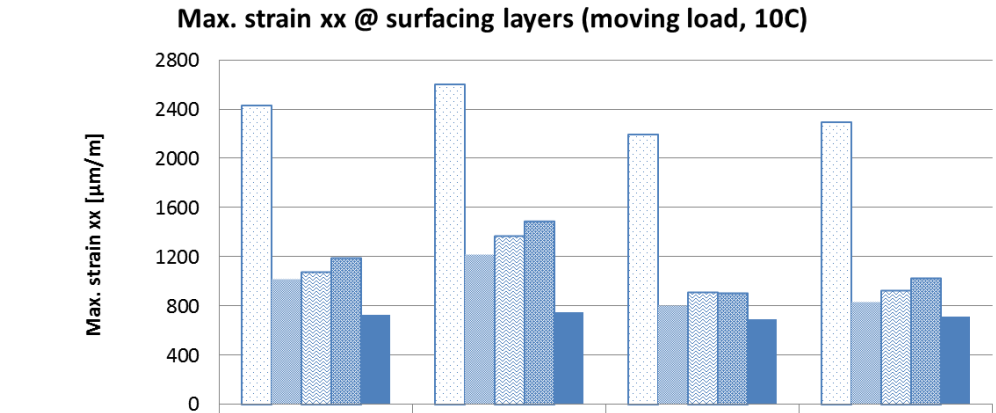

	surf.1	surf.2	surf.3	surf.4
Max. strain xx @ PA	2432	2604	2197	2298
Max. strain xx @ UM	1019	1217	805	835
Max. strain xx @ GA	1079	1368	912	924
Max. strain xx @ BM	1193	1489	904	1028
Max. strain xx @ ST	729	750	688	712

Figure 12 Max. transversal strain ε_{xx} at material layers of four surfacing systems (+10 °C)

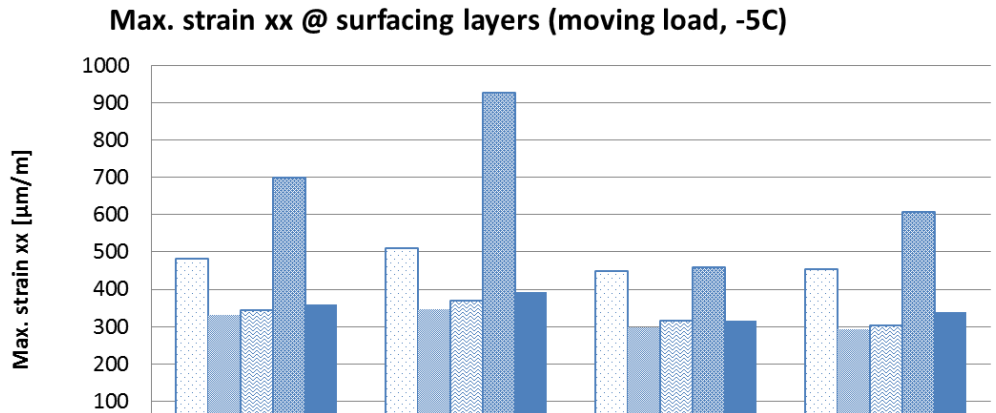

	surf.1	surf.2	surf.3	surf.4
Max. strain xx @ PA	482	509	449	453
Max. strain xx @ UM	330	347	298	292
Max. strain xx @ GA	345	370	315	302
Max. strain xx @ BM	700	925	457	608
Max. strain xx @ ST	358	392	315	339

Figure 13 Max. transversal strain ε_{xx} at material layers of four surfacing systems (-5 °C)

From Figure 12 & 13 the following observations need to be addressed:

- At 10°C, the maximum tensile transversal strain occurs on the top of PA in the surfacing structure 2. The maximum tensile transversal strain at -5°C occurs on the bottom membrane

in the surfacing structure 2. At 10°C and -5°C, the lower tensile transversal strains appear on all layers in the surfacing structure 3 and 4.

- The maximum tensile normal strains occur at the both temperatures of 10°C and -5°C, on the bottom membranes in the surfacing structure 2.
- The maximum longitudinal tensile strains occur at 10°C, on the top of PA in the surfacing structure 2. However, at 10°C and -5°C, the four surfacing structures show almost the same magnitude of longitudinal tensile strain on the top of PA layer and steel deck. The lower temperature (-5°C) has less influence on development the longitudinal tensile strain.
- At 10°C, the higher shear strains are developed on the upper and the bottom membranes in the surfacing structure 2. However, at 10°C and -5°C, the lower shear strains occur always on the upper and bottom membrane in the surfacing structure 3.

3.3 Evolution of the total damage in surfacing materials

The evolution of damage in the surfacing structure 1 that results from a dual-wheel moving load, at temperatures +10°C and loading speeds 80km/h after 1000 cycles is shown in Figure 14.

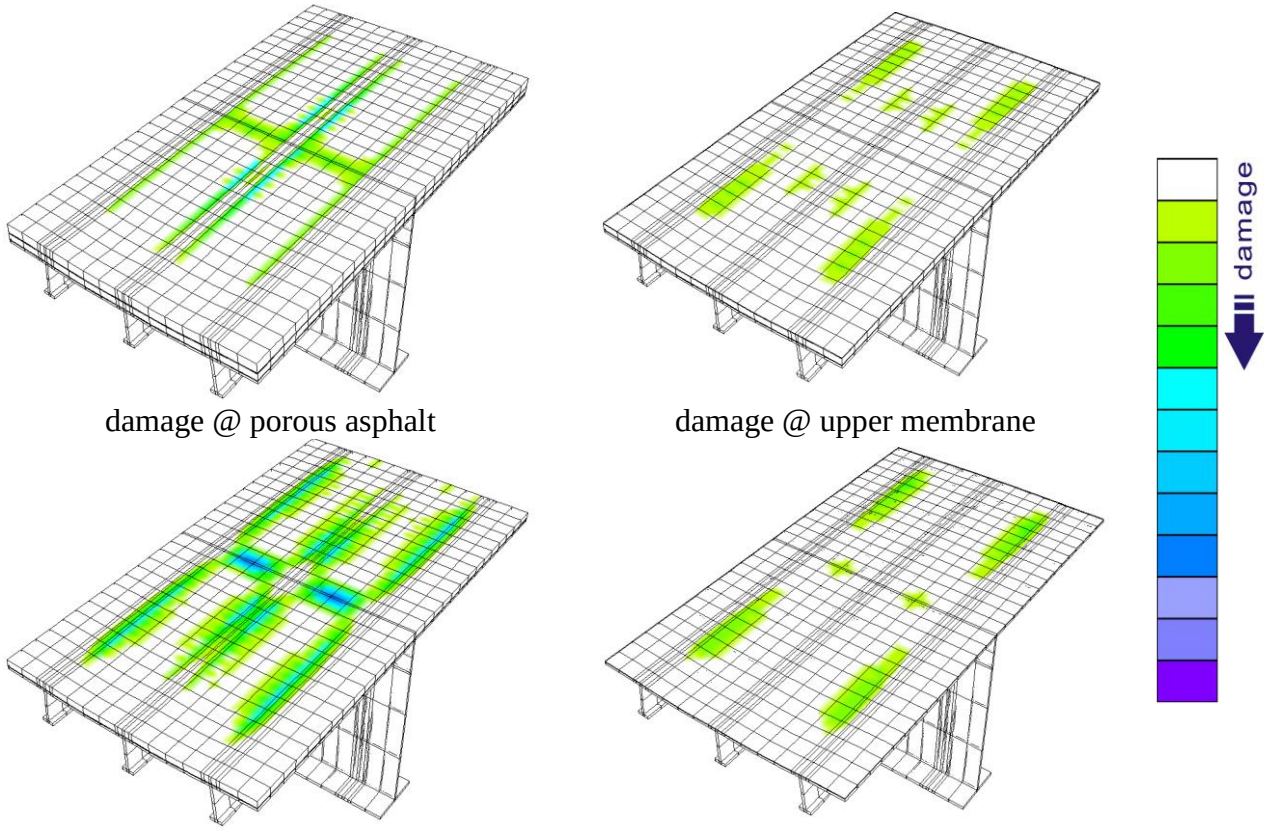

Figure 14 Damage distributions in surfacing layers after moving load of 1000 cycles (10°C)

Figure 14 gives a global impression of the distribution of the damage in the surfacing structure 1 due to the passage of the moving load. The following remarks can be drawn.

- As expected, the total damage at the surfacing layers on the steel deck increases after each load cycle.
- The damage follows more or less the wheel paths.
- The damage accumulation under the wheel that travels over the stiffener is much larger than that under the wheel travels between two stiffeners. This can be understood by considering the fact that the crossbeam supports the steel plate between the stiffeners and does not support the steel plate over the stiffeners.

- The highest total damages occur in GA layer at the cross beam and at the midway between two successive crossbeams, where also the stresses and strains are highest.

4 REMARKS AND CONCLUSIONS

The following remarks and conclusions can be drawn from FE simulations of the aforementioned cases:

- The multilayer surfacing structure does not behave as a fully bonded composite beam because of the influence of the shear stiffness of the membrane materials and the bonding characteristics of the membrane
- The distribution of the strains along the depth of the surfacing structure is not linear. This is also noticed by simulation work done by Liu et al.[5] and experimental work carried out by Hamaue et al.[6].
- The response of the surfacing structure differs significantly at different temperatures due to the high temperature sensitivity of asphaltic materials.
- The transversal strains in all material layers are considerably higher than the longitudinal strains due to the under-deck steel stiffeners in the longitudinal direction. This is also the reason why most of the reported cracks in the surfacing structure on orthotropic steel bridges are along the longitudinal direction.
- The membrane layers undergo quite high shear deformations and play an important role in ensuring the integrity of the bridge deck surfacing. It is extremely important to use a membrane product with good bonding characteristics in order to obtain good composite behavior of the surfacing.
- The surfacing structure 3 shows the better integral response than the other three surfacing structures. The surfacing structure 1 and 4 can be recommend as second option. However the surfacing structure 2 is not recommend for the Dutch OSDB.

ACKNOWLEDGEMENT

This research project is funded by the Dutch Transport Research Centre (DVS) of the Ministry of Transport, Public Works and Water Management (RWS). Their financial support is highly appreciated.

REFERENCES

[1] Gurney, T. “Fatigue of Steel Bridge Decks,” Transport Research Laboratory, Department of Transport, HMSO Publication Centre, London, England, 1992.

[2] Wang, C., Feng, Y., and Duan, L., 2009. Fatigue damage evaluation and retrofit of steel orthotropic bridge decks. Key Engineering Materials, Vols. 413-414, pp 741-748. Switzerland: Trans Tech Publications.

[3] Scarpas, A. & Liu, X. "CAPA-3D Finite Elements System User's Manual, parts I, II and III," Department of Structural Mechanics, Faculty of Civil Engineering, Delft University of Technology, Delft, The Netherlands, 2008.

[4] Liu, X., Scarpas, A., “Experimental and Numerical Characterization of Membrane Adhesive Bonding Strength on Orthotropic Steel Deck Bridges”, Report, Delft University of Technology, The Netherlands, 2012.

[5] Liu, X., Medani, T.O., Scarpas, A., Huurman, M. and Molenaar, A.A.A. "Experimental and numerical characterization of a membrane material for orthotropic steel deck bridges: Part 2-Development and implementation of a nonlinear constitutive model," Finite Elements in Analysis and Design, vol. 44, pp. 580-594, June 2008.

[6] Hameau, G., C. Puch, and A.M. Ajour, REVETEMENTS DE CHAUSSEES SUR PLATELAGES METALLIQUES - 2 - COMPORTEMENT A LA FATIGUE EN FLEXION SOUS MOMENT NEGATI, 1981.